



Activated Carbon-Supported BiFeO₃ for Sustainable Dye Degradation

Ceren ORAK ^{1*}, Kübra KÖŞE KAYA ², Sabit HOROZ ^{2,3}

¹ Department of Chemical Engineering, Faculty of Engineering and Natural Sciences, Sivas University of Science and Technology, Sivas, Turkey

² Department of Engineering Fundamental Sciences, Faculty of Engineering and Natural Sciences, Sivas University of Science and Technology, Sivas, Turkey

³ Nanophotonics Research and Application Center (CÜNAM), Sivas, 58140, Turkey

*Sorumlu Yazar (Corresponding author): crn.orak@gmail.com

Abstract

The persistence and toxicity of synthetic dyes in aquatic environments demand innovative and sustainable treatment solutions. This study investigates the photocatalytic degradation of tartrazine using an activated carbon-supported BiFeO₃ (AC/BFO) composite under visible light. The AC/BFO catalyst was characterized using SEM, BET, XRD and FT-IR analyses to confirm its structural and chemical properties. Key reaction parameters, including catalyst loading, hydrogen peroxide concentration, and pH, were optimized to maximize degradation efficiency. The results revealed that a catalyst loading of 0.2 g/L, 10 mM hydrogen peroxide, and pH 3 achieved the highest degradation rate. These findings highlight the potential of AC/BFO composites as effective photocatalysts for dye-laden wastewater treatment, contributing to the advancement of green and sustainable remediation technologies.

Research Article

Article History

Received : 18.04.2025

Accepted: 21.06.2025

Keywords

Photocatalysis,
Activated carbon,
BiFeO₃,
Tartrazine

1. Introduction

The increasing discharge of synthetic dyes into aquatic environments has become a significant environmental concern due to their persistence, toxicity, and potential to bioaccumulate (Haste et al., 2024; Horoz et al., 2024.; Orak, 2024a, 2024b; Orak et al., 2023). Tartrazine, a commonly used azo dye in the food, textile, and pharmaceutical industries, is particularly problematic because of its high stability and resistance to conventional degradation processes. The removal of such pollutants from wastewater requires innovative and efficient treatment methods that minimize environmental impact (Askarniya et al., 2022; Monser and Adhoum, 2009; Orak, 2024c; Reck et al., 2018; Sahnoun and Boutahala, 2018). Photocatalysis has emerged as a promising green technology for the degradation of organic pollutants due to its ability to utilize solar energy and generate reactive species that can break down complex molecules (Arabacı et al., 2024; Bakır and Orak, 2024; Bakır et al., 2024a, 2024b; Orak et al., 2024; Orak and Yüksel, 2021, 2022b, 2022a). Among various photocatalysts, BiFeO₃ has gained attention due to its unique multiferroic properties, narrow bandgap, and ability to harness visible light for photocatalytic reactions. However, the practical application of BiFeO₃ is often hindered by rapid charge recombination and limited surface area, which reduce its overall photocatalytic efficiency (Orak et al., 2016; Orak and Yüksel, 2021; Orak and Yüksel, 2022). To address these limitations, the incorporation of activated carbon as a support material offers a viable strategy. Activated carbon not only provides a high surface area for pollutant adsorption but also facilitates electron transfer and reduces charge recombination. The combination of BiFeO₃ with activated carbon is expected to enhance photocatalytic activity by synergistically

coupling adsorption and degradation mechanisms (Batur et al., 2022; Joshiba et al., 2022; Raizada et al., 2017). This study aims to investigate the photocatalytic degradation of tartrazine using activated carbon-supported BiFeO₃ as a composite photocatalyst. The research focuses on synthesizing and characterizing the composite material, evaluating its photocatalytic performance under visible light irradiation, and optimizing the degradation conditions. The findings of this study are anticipated to contribute to the development of effective and sustainable approaches for the treatment of dye-laden wastewater.

2. Materials and Method

2.1. Catalyst preparation and characterization

The precursors (Bi(NO₃)₃·H₂O, Fe(NO₃)₃·9H₂O, and citric acid) were dissolved in an ethanol-water solution with a Bi:Fe: citric acid molar ratio of 1:1:3. The activated carbon was then incorporated into the mixture to achieve a composite structure with 10 wt.% BFO. The resulting mixture was stirred vigorously and heated until a gel formed. Following drying, the material was calcined at 400 °C for 4 hours and finally, activated carbon supported BiFeO₃ (AC/BFO) was obtained. In the context of characterization study, SEM, FT-IR, XRD and BET analysis were performed.

2.2. Experimental set-up and procedure

The experimental study involved treating a 20 ppm tartrazine solution (100 mL) under visible light (300W Xe lamp) for 1 h. The effects of key reaction parameters, including pH (3–9), catalyst concentration (0–0.4 g/L), and initial hydrogen peroxide concentration (0–20 mM), were examined. Liquid samples were collected at the end of each experiment and analyzed using a spectrophotometer. The degradation process was assessed by monitoring the breakdown of aromatic rings in tartrazine molecules and the efficiencies of this process were calculated using the given equation:

$$\% \text{ Degradation of tartrazine} = \frac{A_{0at\ 258nm} - A_{t\ at\ 258nm}}{A_{t\ at\ 390nm}} \times 100$$

3. Results and Discussion

3.1. Characterization study

The structural and functional integrity of AC/BFO composite was assessed using SEM and FT-IR analyses, as depicted in Figure 1. The SEM image (Figure 1a) reveals a highly porous structure, where BFO nanoparticles are uniformly distributed over the activated carbon (AC) framework. The nanoscale dispersion of BFO increases the composite's surface area, providing more active sites for adsorption and photocatalytic reactions. The pores in AC likely contribute to improved mass transfer of reactants, enhancing catalytic performance. Also, BET areas of BFO, AC and AC/BFO were found as 8.45, 1124.67, and 995 m²/g. The BET surface area analysis revealed that pure BFO exhibited a relatively low surface area of 8.45 m²/g, which is consistent with its non-porous nature. In contrast, AC showed a significantly higher surface area of 1124.67 m²/g due to its highly porous structure and large adsorption capacity. The AC/BFO composite demonstrated a surface area of 995 m²/g, which, while slightly lower than that of pure AC, still represents a substantial improvement compared to BFO alone. This result confirms that the incorporation of AC into the composite significantly enhances the overall surface area, thereby providing more active sites for adsorption and photocatalytic reactions. The slight reduction in surface area compared to pure AC is attributed to the partial coverage of AC pores by BFO particles, yet the composite retains excellent textural properties favorable for photocatalysis.

The FT-IR spectrum (Figure 1b) confirms the successful synthesis of the AC/BFO composite. Peaks at approximately 550–600 cm^{-1} correspond to Bi-O and Fe-O stretching vibrations, characteristic peaks of BFO (Hussain et al., 2013; Orak and Aslı Yüksel, 2022b, 2022a). Additional peaks in the range of 1000–1300 cm^{-1} are attributed to functional groups present in AC, such as C–O stretching (Batur et al., 2023; Jain, Balasubramanian, and Srinivasan, 2016). The presence of these peaks verifies the integration of AC with BFO, suggesting strong interaction between the components, which can mitigate charge recombination and enhance photocatalytic efficiency. Based on the XRD patterns presented in Figure 1(c) and (d), the crystallographic structures of AC, BFO, and AC/BFO were compared. As shown in Figure 1(c), the pure BFO sample exhibits sharp and distinct diffraction peaks corresponding to the rhombohedral perovskite phase of BFO, indicating its high crystallinity. In the AC/BFO composite, the main diffraction peaks of BFO are still clearly visible, suggesting that the crystalline structure of BFO remains intact after the incorporation of activated carbon. However, a slight reduction in peak intensity and minor broadening are observed, likely due to the presence of amorphous carbon surrounding the BFO particles. Figure 1(d) shows the XRD pattern of pure activated carbon, which displays two broad peaks centered around $2\theta \approx 24^\circ$ and 43° , corresponding to the (002) and (100) planes of disordered graphite-like carbon. These broad peaks confirm the amorphous nature of AC. The co-existence of crystalline BFO peaks with amorphous carbon features in the AC/BFO pattern confirms the successful formation of the composite without significant disruption to the BFO crystal structure (Hussain et al., 2013; Rusevova et al., 2014). According to previous studies, pure BFO typically shows a relatively strong PL emission, which is associated with rapid recombination of photo-induced electron–hole pairs. In contrast, the incorporation of AC significantly suppresses the PL intensity in AC/BFO composites. This reduction in emission is commonly interpreted as an indication of enhanced charge separation efficiency and reduced recombination rate, which ultimately contribute to improved photocatalytic performance (Soltani and Lee, 2017; Tanapongpisit et al., 2024).

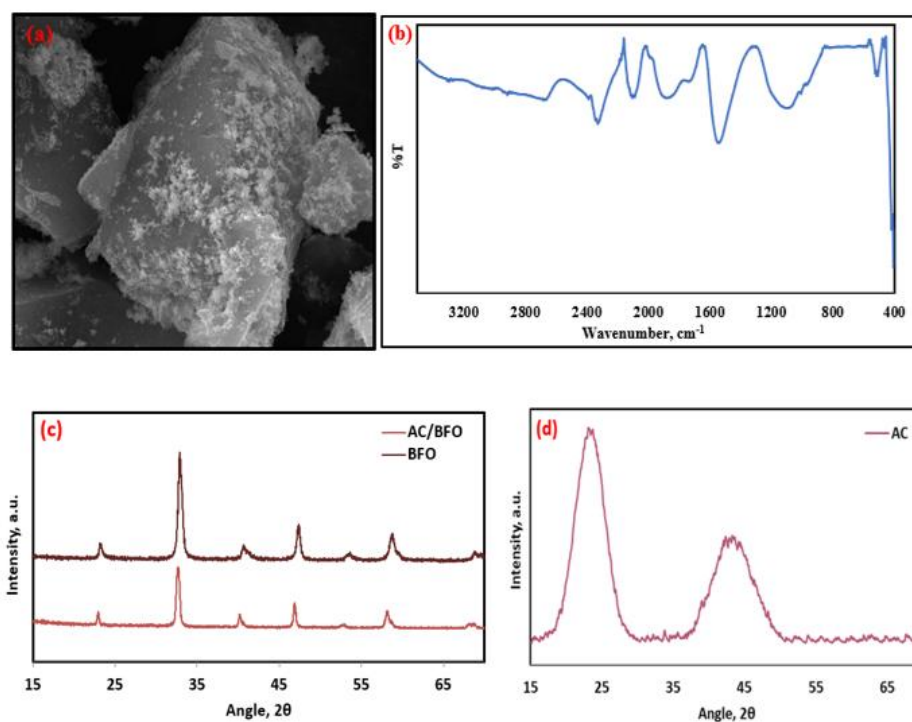


Figure 1. (a) SEM image of AC/BFO, (b) FT-IR spectrum of AC/BFO, (c) XRD diagram of BFO and AC/BFO and (d) XRD diagram of AC.

3.2. Photocatalytic degradation of tartrazine

The photocatalytic performance of AC/BFO was systematically evaluated by investigating the impacts of catalyst loading, initial hydrogen peroxide concentration (HPC), and pH on the degradation of tartrazine under visible light, as illustrated in Figure 2. As depicted in Figure 2a, the photocatalytic degradation efficiency increased with higher catalyst loading and this improvement is attributed to the greater availability of active sites on BFO and the enhanced adsorption capacity provided by AC. However, beyond the optimal loading (0.2 g/L), the efficiency slightly increased, likely due to light scattering and shielding effects caused by excessive catalyst particles in the tartrazine solution. These phenomena reduce the penetration of visible light, limiting photocatalytic activity (Gupta et al., 2011; Cao et al., 2022). Figure 2b illustrates the effect of HPC on the photocatalytic degradation efficiency of tartrazine. The results show a consistent increase in degradation efficiency as HPC rises from 0 to 20 mM. At low HPC (0–10 mM), the degradation efficiency improves significantly. Hydrogen peroxide (HP) acts as an electron acceptor, reducing charge recombination in the photocatalyst. This reaction generates reactive oxygen species (ROS), such as hydroxyl radicals ($\bullet\text{OH}$), which are highly effective at breaking down tartrazine molecules. The maximum degradation efficiency is achieved around 10 mM of HPC. At this point, there is an optimal balance between the generation of reactive radicals and the availability of tartrazine molecules for reaction. At higher concentrations (20 mM), the degradation efficiency decreases. This phenomenon occurs because excessive HP can act as a scavenger of hydroxyl radicals (Nisar et al., 2020; Sun et al., 2020; Wu and Chern, 2006; Orak and Ersöz, 2024; Arabacı et al., 2025). The pH of the tartrazine solution significantly influenced photocatalytic efficiency, with maximum degradation observed at pH 3, as illustrated in Figure 2c. This can be attributed to the ionization state of the dye molecules and the surface charge of the catalyst. Under slightly acidic conditions, tartrazine molecules are more prone to adsorption on the positively charged catalyst surface, promoting their degradation. In highly acidic or alkaline environments, the interaction between the dye and the catalyst weakens due to electrostatic repulsion or changes in the chemical stability of the photocatalyst (Rahman et al., 2013; Van et al., 2020). As a conclusion, the catalyst loading of 0.2 g/L, 10 mM of HPC, and pH 3 were identified as the optimal conditions for maximum degradation efficiency (almost %90). At the same reaction conditions, the degradation performance of BFO alone was tested to better illustrate the synergistic effect of the AC/BFO composite. The results showed that using only BFO resulted in a degradation efficiency of 78.3%, which is notably lower than the ~90% efficiency observed with the AC/BFO. This comparison confirms that the incorporation of AC significantly enhances the photocatalytic activity, likely due to its high adsorption capacity and its role in facilitating charge separation and suppressing electron-hole recombination.

Based on similar studies in the literature, the degradation mechanism primarily involves the generation of reactive oxygen species (ROS), such as hydroxyl radicals ($\bullet\text{OH}$) and superoxide anions ($\bullet\text{O}_2^-$), upon visible light excitation of AC/BFO. When AC/BFO is irradiated, electron-hole pairs are generated. The photogenerated electrons (e^-) in the conduction band react with dissolved oxygen to form $\bullet\text{O}_2^-$ radicals, while holes (h^+) in the valence band oxidize water or hydroxide ions to generate $\bullet\text{OH}$ radicals. These highly reactive species attack the azo bonds ($-\text{N}=\text{N}-$) and aromatic structures of tartrazine, leading to successive decolorization and mineralization into CO_2 , H_2O , and inorganic ions. The role of activated carbon is crucial in enhancing adsorption of dye molecules and facilitating electron transfer, which suppresses charge recombination and boosts ROS formation. This synergistic effect between BFO and AC improves the overall degradation efficiency. Relevant studies such as those by Rana et al. (2024) and Ponraj et al. (2017) support this proposed mechanism (Ponraj and Daniel, 2017; Rana et al., 2024).

After five consecutive usage, the AC/BFO catalyst retained almost 92.7% of its original photocatalytic efficiency, demonstrating excellent stability and reusability. This high level of performance preservation indicates that the structural and functional integrity of the composite catalyst remains largely unaffected throughout repeated cycles. The strong interaction between BFO and AC likely contributes to this durability by minimizing catalyst leaching and maintaining active surface sites. These findings confirm the potential of AC/BFO as a reliable and sustainable photocatalyst for long-term applications in dye-contaminated wastewater treatment.

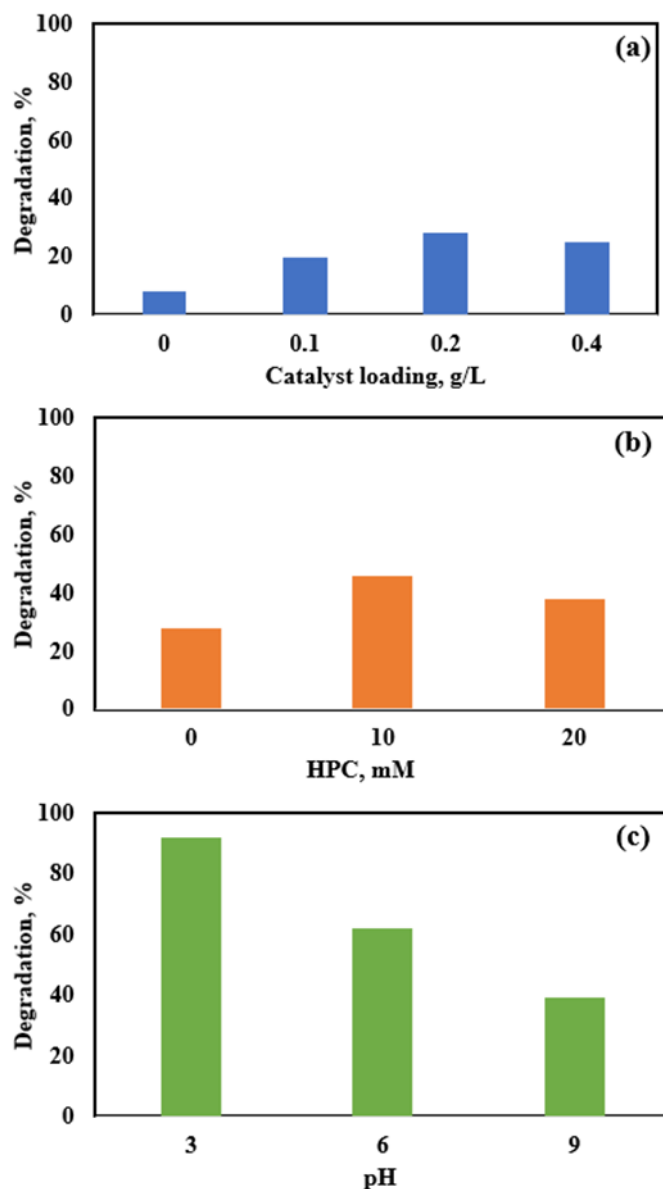


Figure 2. The effect of reaction parameters: (a) catalyst loading, (b) initial hydrogen peroxide concentration, (c) pH.

4. Conclusion

This study successfully demonstrated the synthesis and application of an AC/BFO composite for the photocatalytic degradation of tartrazine under visible light. SEM and FT-IR analyses confirmed the structural integrity and successful integration of AC and BFO, providing a high surface area and effective active sites for photocatalysis. Catalyst loading of 0.2 g/L provided maximum degradation efficiency, balancing active site availability and light

penetration. HPC of 10 mM optimized the generation of hydroxyl radicals without observing scavenging effect. A pH of 3 created favourable conditions for dye adsorption and photocatalytic reactions. Overall, the AC/BFO composite exhibited high efficiency in degrading tartrazine, demonstrating its promise as a sustainable photocatalyst for environmental remediation.

References

- Arabacı, B., Bakır, R., Orak, C., Yüksel, A., 2024. Integrating experimental and machine learning approaches for predictive analysis of photocatalytic hydrogen evolution using Cu/g-C₃N₄. *Renewable Energy*, 237: 121737.
- Arabacı, B., Bakır, R., Orak, C., Yüksel, A., 2025. Predictive modeling of photocatalytic hydrogen production: integrating experimental insights with machine learning on Fe/g-C₃N₄ catalysts. *Industrial & Engineering Chemistry Research*, 64(10): 5184–99.
- Askarniya, Z., Soroush, B., Shirish, H., Sonawane Grzegorz B., 2022. A Comparative Study on the Decolorization of Tartrazine, Ponceau 4R, and Coomassie Brilliant Blue Using Persulfate and Hydrogen Peroxide Based Advanced Oxidation Processes Combined with Hydrodynamic Cavitation. *Chemical Engineering and Processing - Process Intensification* 181.
- Bakır, R., Orak, C., 2024. Stacked machine learning approach for predicting evolved hydrogen from sugar industry wastewater. *International Journal of Hydrogen Energy*, 85: 75–87.
- Bakır, R., Orak, C., Yüksel, A., 2024a. A machine learning ensemble approach for predicting solar-sensitive hybrid photocatalysts on hydrogen evolution. *Physica Scripta*, 99(7): 076015.
- Bakır, R., Orak, C., Yüksel, A., 2024b. Optimizing hydrogen evolution prediction: a unified approach using random forests, lightgbm, and bagging regressor ensemble model. *International Journal of Hydrogen Energy*, 67: 101–10.
- Batur, E., Orhan, B., Sabit, H., Şahin, Ö., Kutluay, S., 2022. Enhancement in incident photon-to-current conversion efficiency of manganese-decorated activated carbon-supported cadmium sulfide nanocomposite. *Journal of Materials Science: Materials in Electronics* 33(20): 16286–96.
- Batur, E., Şahin, Ö., Orhan, B., Sabit, H., Kutluay, S., 2023. High solar cell efficiency of lanthanum-alloyed activated carbon-supported cadmium sulfide as a promising semiconductor nanomaterial. *Journal of the Australian Ceramic Society*, 59(1): 9–18.
- Cao, Y., Guanqing, Y., Ying, G., Xuelian, H., Guozhen, F., Shuo, W., 2022. Facile synthesis of tio₂/g-c₃n₄ nanosheet heterojunctions for efficient photocatalytic degradation of tartrazine under simulated sunlight. *Applied Surface Science*, 600.
- Gupta Vinod K., Rajeev J., Arunima, N., Shilpi, A., Meenakshi, S., 2011. Removal of the hazardous dye-tartrazine by photodegradation on titanium dioxide surface. *Materials Science and Engineering C*, 31(5):1062–67.
- Haste, Z.Ö., Horoz, S., Orak, C., Biçer, E., 2024. Green-Synthesized SnO₂ derived from kombucha tea and assessment of its photocatalytic activity for the degradation of procion red MX-5B. *ChemistrySelect*, 9(43): e202403264.
- Horoz, S., Orak, C., Biçer, E., 2024. Green synthesis of ZnO and Ni-Doped ZnO from okra stalks for the photocatalytic degradation of procion red MX-5B. *International Journal of Phytoremediation*, 1–9.

- Hussain, T.S.A., Siddiqi, S.A., Awan, M.S., 2013. Induced modifications in the properties of sr doped BiFeO₃ multiferroics. *Progress in Natural Science: Materials International* 23(5):487–92.
- Jain, A., Rajasekhar, B., Srinivasan, M.P., 2016. Hydrothermal conversion of biomass waste to activated carbon with high porosity: a review. *Chemical Engineering Journal*, 283:789–805.
- Joshiba, G.J., Kumar, P.S., Rangasamy, G., Ngueagni, P.T., Pooja, G., Balji, G.B., ... El-Serehy, H.A., 2022. Iron doped activated carbon for effective removal of tartrazine and methylene blue dye from the aquatic systems: Kinetics, isotherms, thermodynamics and desorption studies. *Environmental Research*, 215: 114317.
- Monser, L., Nafaâ, A., 2009. Tartrazine modified activated carbon for the removal of Pb(II), Cd(II) and Cr(III). *Journal of Hazardous Materials*, 161(1): 263–69.
- Nisar, A., Muhammad, S., Muhammad, U., Majid, M., Muhammad, A., Iltaf K., Javaid, A., 2020. Kinetic modeling of ZnO-RGO catalyzed degradation of methylene blue. *International Journal of Chemical Kinetics*, 52(10): 645–54.
- Orak, C., 2024a. Application of response surface methodology for bioenergy generation in a yeast-based microbial fuel cell. *RSC Advances*, 14(46): 34356–61.
- Orak, C., 2024b. Enhanced degradation of procion red MX-5B Using Fe-doped corn cob ash and fe-doped g-C₃N₄. *Energy Sources, Part A: Recovery, Utilization, and Environmental Effects*, 46(1): 14244–58.
- Orak, C., 2024c. Treatment of sugar industry wastewater via fenton oxidation with zero-valent iron. *Cumhuriyet Science Journal*, 45(1): 100–104.
- Orak, C., Atalay, S., Ersöz, G., 2016. Degradation of Ethylparaben Using Photo-Fenton-like Oxidation over BiFeO₃. *Anadolu University Journal Of Science And Technology A - Applied Sciences and Engineering*, 17(5): 915–915.